ISSN 0018-151X, High Temperature, 2020, Vol. 58, No. 4, pp. 595–614. © Pleiades Publishing, Ltd., 2020.
Russian Text © The Author(s), 2020, published in Teplofizika Vysokikh Temperatur, 2020, Vol. 58, No. 4, pp. 646–669.

HEAT AND MASS TRANSFER AND PHYSICAL GASDYNAMICS

Two-Phase Flows with Solid Particles, Droplets, and Bubbles: Problems and Research Results (Review)

A. Yu. Varaksin[a, b, *]

[a]*Joint Institute for High Temperatures, Russian Academy of Sciences, Moscow, Russia*
[b]*Bauman Moscow State Technical University, Moscow, Russia*
**e-mail: varaksin_a@mail.ru*

Received March 5, 2020; revised March 10, 2020; accepted March 10, 2020

Abstract—The computational-theoretical and experimental works on different types of two-phase flows are reviewed. The problems of two-phase flows and features of their study are considered. The basic characteristics of two-phase flows and the methods of their simulation are provided. The results of the study of two-phase flows with solid particles, droplets, and bubbles are outlined and analyzed.

DOI: 10.1134/S0018151X20040161

CONTENTS

INTRODUCTION

The flows of a medium carrying a disperse admixture in the form of solid particles, droplets, or bubbles take place in a series of natural phenomena: tornados [1], dust storms, volcanic eruptions, wildfires, precipitation in the form of hail, show, rain, different types of fog, gas liberation in seas and oceans, etc. Typical examples of technical facilities with two-phase flows include the combustion chambers of thermal engines, the paths of solid- and liquid-propellant reaction engines, facilities for the thermal pretreatment of coal in schemes for the power-engineering use of fuel, steam generators, firefighting systems, heat exchangers with two-phase working bodies, sand- and bead-blasting facilities with different surfaces, pneumatic conveyors of granular materials, dust collectors of different types, and many others.

The main types of two-phase (heterogeneous) systems are gas–solid particles, gas–droplets, liquid–solid particles, and liquid–bubbles.

The interest of many research groups around the world regarding research on two-phase (multiphase, heterogeneous) flows has steadily increased in recent decades.

In the 60 years of the existence of the Joint Institute for High Temperatures of the Russian Academy of Sciences, its researchers have published hundreds of original and pioneering works on particular aspects of fluid and gas dynamics and the thermal physics of multiphase flows. Many of them were printed in the journal *High Temperature* (*Teplofizika vysokikh temperatur*). Therefore, the current review, which describes the most important achievements in the research on two-phase flows, is deservedly focused on works recently published in this journal by researchers of the Joint Institute for High Temperatures of the Russian Academy of Sciences and their colleagues from other institutions.

1. PROBLEMS AND FEATURES OF THE STUDY OF TWO-PHASE FLOWS

The research on two-phase (heterogeneous) flows is intended to solve two main classes of problems [2].

The first problem (or the direct one) consists of the study of the behavior of a disperse admixture (particles, droplets, or bubbles) in the flow of a carrier medium (gas or liquid). The solution to this problem lies in the determination of the characteristics of disperse inclusions, i.e., their sizes (in the case of polydisperse flow or presence of phase and/or chemical transformations), the fields of their averaged and fluctuation (mean square) velocities and temperatures, their concentrations, etc.

The second problem (or the inverse one) consists of the study of the effect of the disperse phase on the flow characteristics of the media carrying it. To solve this problem, it is necessary to determine the characteristics of the gas (liquid) in the presence of particles (droplets or bubbles), i.e., the fields of averaged and fluctuation (mean square) velocities and temperatures, friction coefficients, heat dissipation, etc.

The study of two-phase (multiphase) flows is extremely difficult, which is probably associated with two circumstances. On the one hand, the theory of single-phase flows (especially turbulent flows) is in the developmental stage. On the other hand, the addition of a disperse admixture in the form of particles (droplets and bubbles) makes the flow pattern significantly more complex. It is related to a wide variety of properties (primarily, inertia) and the concentration of disperse inclusions, which leads to multiple modes (classes) of two-phase flows.

To confirm this, w some features of the study of two-phase flows are given below.

1.1. Multiscale Character

Inertia (which is primarily determined by size and density) of the disperse phase may vary over an immense range (many orders of magnitude). Single-phase flows are characterized by several spatial and temporal scales determined by the value of the flow velocity inherent to them, the flow regime (laminar, transient, or turbulent), the flow geometry, etc. [2]. To model the motion of disperse phase correctly, one must take into account its interaction at different scales, which is determined by (i) the averaged motion, (ii) large-scale fluctuation motion, (iii) small-scale fluctuation motion, (iv) various instabilities (for instance, the Tollmien–Schlichting instability in boundary layers, the Taylor–Gertler instability in pipes, and the Kelvin–Helmholtz instability in pure shear layers), etc.

1.2. Multiplicity of Force Factors

To integrate the equations of motion of the disperse phase (particles, droplets, or bubbles) correctly, a large number of force factors (forces) must be taken into account. The main forces include (i) the aerodynamic drag force, (ii) the gravitational force (buoyancy), (iii) the Saffman force, (iv) the Magnus force, (v) the thermophoretic force, (vi) the turbophoretic force, (vii) the diffusiophoretic force, (viii) the centripetal force, (ix) the electrostatic force, and (x) the near-wall force.

It is worth noting that many of the forces mentioned above somehow contain the velocity of the carrier phase, which is a random variable in a turbulent stream. Therefore, a question is often raised about the applicability of a specific expression to calculate force under other conditions (e.g., for laminar flow or without speed shear).

1.3. Multiplicity of Modeling Parameters

The mathematical or physical modeling of single-phase flows involves the calculation or measurement of a sufficiently large number of parameters (or their spatial distributions).

In the case of a non-isothermal, stationary, turbulent, single-phase flow, these parameters include (i) three components of the average velocity, (ii) three components of the fluctuation (mean square) velocity, (iii) the average temperature, (iv) the fluctuation (mean square) temperature, (v) binary correlations of various components of the fluctuation velocities (components of the Reynolds stress tensor), (vi) binary correlations of the fluctuation velocity and fluctuation temperature, etc.

For the mathematical and physical modeling of two-phase flows containing particles, droplets, or bubbles, the number of necessary parameters increases by many times, because the aforementioned parameters are supplemented by analogous parameters for the disperse phase (e.g., the average and fluctuation velocities and temperatures of particles, etc.), including its size, size distribution, and the averaged and fluctuating concentration (gas content), as well as the parameters for the carrier phase (already with disperse inclusions), which include the phase-transition heat and many others.

1.4. Presence of Different Collision Processes

Various collision processes may occur in two-phase (multiphase) flows [3]. These include (i) interaction between disperse inclusions (particle–particle, droplet–droplet, or bubble–bubble), (ii) interaction between disperse inclusions and a rigid body streamlined by the two-phase flow (particle–body, droplet–body, or bubble–body), and (iii) interaction between a disperse admixture and the walls restricting the two-phase flow (particle–wall, droplet–wall, or bubble–wall). The first process takes place upon the collision of disperse inclusions with sizes on the same order of magnitude, the second process occurs when the dimensions of the rigid body are many orders of magnitude larger, and the third process occurs place when the dimension (the curvature radius) of the streamlined body tends to infinity, i.e., it degenerates into a flat wall.

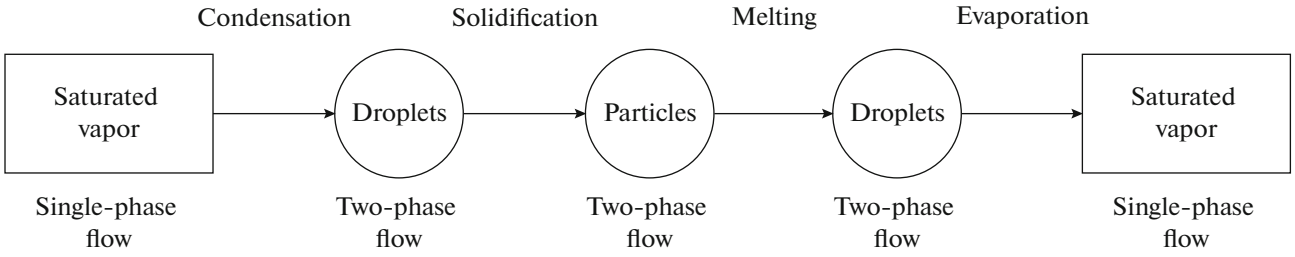

Fig. 1. Role of phase transformation upon the transition of the system from the single-phase state to the two-phase state and vice versa.

Let us list the main reasons for the appearance of collisions among disperse phase items (particles, droplets, or bubbles): (i) a polydisperse character (an admixture of different sizes), which leads to the appearance of different average velocities, (ii) the effect of the average velocity gradient of the carrier phase, (iii) the effect of the gravitational force (of the buoyant force), (iv) the turbulent transport effect, which implies the appearance of the relative velocity between the neighboring particles, (v) the clusterization effect, i.e., an increase in the concentration (gas content) of the disperse phase in local spatial regions, (vi) electrostatic interaction, and (vii) Brownian motion.

Collision interactions may lead to coagulation and fragmentation processes, which significantly affect the dispersed content of the admixture and the generation of films and streamlets on streamlined surfaces. We may conclude that all of the aforementioned collision processes play a considerable role in the formation of statistical characteristics of thee motion of particles (droplets or bubbles) and, consequently, influence the flow characteristics of the carrier continuum. Hence, the study of contact interaction in the context of the two main problems in the study of two-phase flows is highly topical.

1.5. Presence of Phase and Chemical Transformations

We must separately point out the special role of various phase transformations in fluid and gas dynamics and the thermal physics of two-phase (multiphase) flows. The main phase transformations are well-known: (i) condensation, (ii) solidification, (iii) melting, (iv) vaporization (boiling), and (v) sublimation.

The presence of phase transformations often promotes the transformation of an originally single-phase flow to a two-phase one and vice versa (see Fig. 1) and leads to the transition of a two-phase flow from one type to the other. Let us provide some examples.

Bubbles are generated in originally single-phase liquid during boiling, whereas the collapse (disappearance) of bubbles occurs due to vapor condensation in them and returns the system to the single-phase state.

The melting of particles in a gas flow leads to the transition of a two-phase, gas–solid particle flow to a gas–droplet flow. The subsequent crystallization (solidification) of droplets may cause a return to the original state.

The processes of water-vapor condensation on droplets lead to variation in their size and inertia, which may cause a qualitative restructuring of the two-phase flow. The evaporation of moving droplets from the surface also significantly affects the characteristics of the motion of both the disperse phase and the entire two-phase flow as a whole.

Combustion holds a special place among chemical transformations. The combustion processes of fuel liquid droplets and solid particles are of great importance in various engineering applications. Some other examples of chemical reactions that lead to the transition of a system from the single-phase state to the two-phase one and vice versa are the following: (i) gas-bubble emission in liquids due to a chemical reaction, (ii) the deposition of solid particles in liquids in the form of sediment, and (iii) the dissolution of solid particles in liquids.

1.6. Multiplicity of Dimensionless Parameters

The complexity and multiplicity of physical phenomena and processes occurring in two-phase flows lead to the appearance of a large number of additional (compared to single-phase flows) dimensionless parameters (criteria) responsible for the presence and intensity of a particular process. The main parameters are (i) the Reynolds numbers of the particle, droplet, and bubble (Re_p, Re_d, and Re_b), which is constructed from the diameter of the disperse phase and the velocity difference (dynamic sliding) between the phases, (ii) the Stokes numbers in the averaged, large-scale pulsation, and small-scale fluctuation motions (Stk_f, Stk_L, and Stk_K), (iii) the collisional Stokes numbers (Stk_c and $\mathrm{Stk}_{\mathrm{cw}}$), which characterize the inertia of the disperse phase with respect to interparticle collisions and collisions with the channel wall, (iv) the Weber number We, and many others.

Note that, when we consider non-isothermal two-phase flows, we need to introduce the corresponding

dimensionless parameters characterizing the temperature difference (the thermal sliding) between the phases and the thermal inertia of the disperse phase with respect to the corresponding characteristic time scales of temperature variation of the carrier medium.

2. MODERN METHODS FOR THE MODELING OF TWO-PHASE FLOWS

When the motion of a disperse admixture formed by solid particles (droplets or bubbles) and its inverse effect on the characteristics of the carrier continuum (gas or liquid) are studied, the methods of mathematical modeling are of crucial importance. The multiple flow regimes of two-phase media, a classification of which was attempted in work [4], led to the creation of a huge number of mathematical models of such flows.

The whole range of mathematical models developed to date can be conventionally divided into two large classes (types). The models of the first class (Eulerian–Lagrangian, trajectory, and stochastic models) consist of the solution of the equations of motion of the carrier phase in the usual Eulerian formulation, whereas the motion of particles (droplets or bubbles) is described by the Lagrange equations integrated along their trajectories. The models of the second class (Eulerian–Eulerian, continuum, and two-liquid models) describe the motion of the carrier phase and the motion of multiple disperse inclusions based on the Eulerian continual representation.

We briefly consider the advantages and limitations of the Eulerian–Lagrangian and Eulerian–Eulerian models to describe the flow motion of continua with solid particles, droplets, and bubbles [5].

The great advantage of Eulerian–Lagrangian (trajectory or stochastic) models is that they give detailed statistical information on the motion of individual particles (droplets or bubbles) as a result of the integration of the equations of motion (of the heat transfer) of the disperse phase in the known (preliminary computed) field of averaged velocities (temperatures) of the carrier phase. To account for the random (pulsation) motion of disperse inclusions caused by their interaction with turbulent vortices of the carrier gas, the stochastic equations of the Langevin type along the trajectories of individual particles (droplets) must be integrated with subsequent averaging of solutions over the ensemble of initial data. This leads to a considerable increase in the computational cost, because a sufficiently representative ensemble of realizations is required to obtain statistically reliable information. As the size of the disperse inclusions decreases, the use of trajectory methods to calculate their motion also becomes more difficult, because the interaction between the particles (droplets or bubbles) and the turbulent vortices of the carrier phase of smaller dimensions must be taken into account in order to obtain correct information on the average characteristics of the disperse phase. This circumstance strongly complicates the computation process.

The trajectory of the Lagrangian description of motion and heat transfer of the disperse phase in the turbulent flow based on the solution to the equation for only averaged values (without allowance for its interaction with random fields of gas velocity and temperature fluctuation) is correct in the case of inertial particles. Such particles (droplets) are not involved in the fluctuation motion of the carrier phase, because their relaxation time is much longer than the integral scale of turbulence. This description is justified when the flow is realized with large particles or droplets.

It is worth noting that, as the concentration of disperse phase increases, difficulties arise with the use the Eulerian–Lagrangian models. We may distinguish the two circumstances. First, an increase in the concentration leads to the inverse effect of the disperse inclusions on the parameters of the carrier phase, and the calculations must be carried out in several iterations, which makes the computational procedure more complex. Second, as the concentration increases, the probability of collisions of particles (droplets) with each other also increases, which implies complexity of their trajectories.

The great advantage of Eulerian–Eulerian (continual or two-liquid) models is the use of equations of the same type to describe the motion of continuum and disperse phases within the mechanics of interpenetrating media [5]. This enables the use of extensive experience in the modeling of single-phase turbulent flows and the application of identical numerical methods for the solution of the entire system of equations. The description of the motion of extremely low-inertia particles causes no principal difficulties. As the mass of a particle (droplet) tends to zero, the limit transition to the problem of turbulent diffusion of passive (inertia-less) admixture appears. Note that allowance for the collisions between particles (droplets) within two-liquid models does not lead to such significant growth in the computational cost as it does with the trajectory modeling.

The disadvantages of Eulerian–Eulerian models are some loss of information about the motion of individual particles (droplets or bubbles); the need for a correct description of the interchange of mass, momentum, and heat; and difficulties in imposing the boundary conditions for the disperse phase at the surfaces bounding the flow [5].

An attempt to unify the advantages of the Lagrangian and Eulerian approaches to describe the disperse phase was carried out, e.g., [6], in which the hybrid Lagrangian–Eulerian method was developed.

As the concentration and inertia of the disperse phase increase, the choice between the two models of two-phase flows becomes a hard question. The general tendency is as follows: as the concentration of the admixture increases and its inertia decreases, the

application of the continual Eulerian approach for the description of the dynamics of the disperse phase appears to be beneficial.

2.1. Description of the Motion of Disperse Phase: Lagrangian and Eulerian Approaches

The motion of an individual spherical particle (droplet or bubble) in an arbitrary liquid (gas) medium is described by the equation [7]

$$\begin{aligned}\frac{d\mathbf{v}}{d\tau} &= \frac{3\rho}{4\rho_p d_p} C_D |\mathbf{u}-\mathbf{v}|(\mathbf{u}-\mathbf{v}) + \mathbf{g} \\ &+ \frac{\rho}{\rho_p}\left(\frac{D\mathbf{u}}{D\tau} - \mathbf{g}\right) + C_A \frac{\rho}{\rho_p}\left(\frac{D\mathbf{u}}{D\tau} - \frac{d\mathbf{v}}{d\tau}\right) \\ &+ C_L \frac{\rho}{\rho_p}(\mathbf{u}-\mathbf{v}) \times \mathrm{rot}\mathbf{u},\end{aligned} \quad (1)$$

where τ is the time, $\mathbf{v}$ is the velocity of the particle (droplet or bubble), $\mathbf{u}$ is the velocity of the carrier gas (liquid) flow, ρ and ρ_p are the densities of the carrier gas (liquid) and particle, d_p is the particle (droplet or bubble) diameter, and $\mathbf{g}$ is the gravitational acceleration.

The terms on the right side of Eq. (1) describe the aerodynamic drag force, the gravitational force (the buoyant force), the effect of attached mass, and the lift due to speed shear of the carrier gas (liquid). Note that the force of the attached mass is written for the case of particle motion in a nonviscous liquid, which is used in most theoretical works on the modeling of particle (droplet or bubble) motion in turbulent flows. The coefficients (the correction functions) C_D and C_L in the drag force and lift may depend on the Reynolds number of the flow around a particle (droplet or bubble), the speed shear, and other parameters.

Since the velocity of the liquid $\mathbf{u}$ and its acceleration $D\mathbf{u}/D\tau$ in the turbulent flow are random variables, Eq. (1) is a stochastic equation of the Langevin type. In work [8] the probability density function (PDF) is introduced for the particle distribution in a turbulent flow in order to transition from a dynamic stochastic description of the motion of individual particles (droplets or bubbles) to a continual simulation of an ensemble of particles (droplets or bubbles). After that, from the kinetic equation for the PDF, we can derive the system of equations necessary to model the motion of the disperse phase (of particles, droplets, or bubbles) in the continual Eulerian representation.

It is worth noting that the statistical approach based on the distribution functions in the phase space is a reliable tool for the construction of the theoretical models in different areas of physics. Examples can include the Boltzmann equation and the Bogolyubov–Born–Green–Kirkwood chain of equations in the molecular-kinetic theory of gases and liquids, the Fokker–Planck equation for describing the motion of Brownian particles, the Vlasov kinetic equation in the plasma physics, the Smolukhovskii–Müller equation in the coagulation theory, etc. The statistical approach was first used to describe the pseudo-turbulent flow of a disperse media in paper [9].

2.2. Methods of Direct Numerical Simulation (DNS and LES)

The method of direct numerical simulation (DNS) refers to the solution of the nonstationary Navier–Stokes equations for instantaneous quantities without the introduction of auxiliary closing relations or equations, i.e., without simulation of the turbulence. Using the DNS method for the carrier continuum, together with the Lagrangian stochastic approach for the disperse phase, we can obtain the most detailed information about the structure of the turbulent two-phase flow. With DNS, we describe the entire spectrum of turbulent vortices, including small-scale ones responsible for the dissipation of the turbulence energy. A well-known limitation of this method is its inappropriateness for moderate and large Reynolds numbers, because DNS then requires a long computational time, even if we use the fastest computers.

A variety of this approach is large eddy simulation (LES). In the realization of this method, only large energy-carrying vortices with a spatial scale larger than the mesh-element size are directly simulated [10], whereas the small-scale (subgrid-scale) modes appear to be outside the solvability limits and are described in a semiempirical manner. Thus, an attempt is made to avoid the aforementioned disadvantage and to expand the scope of the method. Note that LES is applicable for the modeling of the behavior of particles (droplets) with a relaxation time that is much longer than the temporal microscale of turbulence [11]. This limitation follows from the requirement that the contribution of the subgrid-scale fluctuations (small-scale turbulence) to the statistics of the disperse phase must be small to negligible.

In the vast majority of earlier studies on two-phase flows with particles (droplets), these two methods were used to model the motion of individual particles. To this end, the trajectories of a large ensemble of particles (droplets) added to the turbulent flow were calculated, and the obtained spatial characteristics of the particles motion were subsequently averaged. In later studies DNS was successfully used to calculate dilute flows with an inverse influence of the particles on the flow characteristics of the carrier phase.

2.3. Methods for the Simulation of Flows with Moving Boundaries

To date, many methods for the calculation of liquid flows with moving boundaries have been developed. The classification of the algorithms of contact-boundary resolution based on the used mesh type has

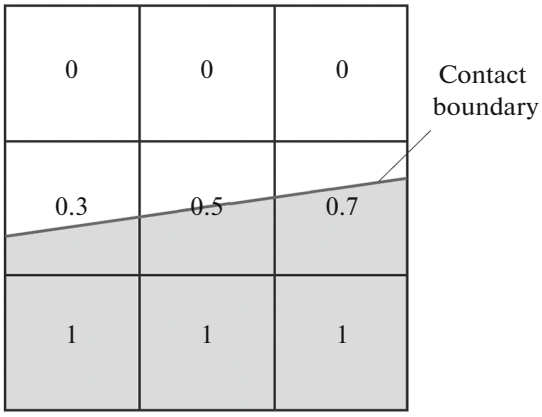

Fig. 2. Schematic representation of a contact boundary with the continuous-marker function in the VOF method [16].

become the most widely used. According to this classification, the algorithms are classified into Lagrangian methods, Eulerian methods, and mesh-free methods. In Lagrangian algorithms the calculation nodes and cells move together with the continuum, whereas the nodes and cells in Eulerian algorithms are at rest and the continuum moves through the Eulerian mesh. In mesh-free methods, either the mesh calculation is not used at all or the mesh is used only to prepare the data for the calculation and analysis of the results.

The Lagrangian method for an incompressible flow [12] is a Lagrangian method, which makes it possible to calculate transient flows of an incompressible liquid with weak deformation of moving boundaries. Another Lagrangian method is the arbitrary Lagrangian–Eulerian method [13], which is a hybrid Eulerian–Lagrangian method. There are three types of Eulerian methods to track the contact boundary: point-tracking methods, interface-tracking methods, and interface-capture methods.

In interface-capture methods, including the method of large particles [14] and the volume-of-fluid (VOF) method [15], the interface is identified from the values of the special-marker functions, which are preserved along the Lagrangian trajectories and are governed by the Eulerian transport equation.

Lastly, we note that the VOF method is extremely widespread today (e.g., [16]). In this method the volume fraction of the liquid in the cell of the mesh calculation α is used as a marker function: the cell is filled with liquid at $\alpha = 1$ and is empty at $\alpha = 0$. The interphase boundary corresponds to the isosurface $\alpha = 0.5$ (Fig. 2).

2.4. Methods of Physical Simulation

In the mechanics of single-phase and two-phase flows, there are several different methods of flow diagnostics, from single-point contact methods to a wide class of contactless methods. The class of contactless methods, which primarily includes optical methods, is, in turn, divided into single-point methods (e.g., laser Doppler anemometry (LDA)) and various modifications of field methods, in particular, those based on visualization of the stroboscopic tracer flow.

The stroboscopic tracer flow visualization is based on the registration of the shift of tracer images, i.e., the particles entering the flow, under their two-fold or multiple pulse illumination and on the subsequent calculation of the instantaneous velocity field in the illuminated region. The history of development of the experimental methods based on this principle goes back several decades. In particular, the stroboscopic visualization method was developed in 1960–1970s at the Institute of Thermophysics of the Siberian Branch of the Russian Academy of Sciences for high-precision measurement in the boundary layer and for the diagnostics of the velocity field in thin liquid films [17]. The use of standard stroboscopes and photo- or cine-film were proposed as light sources and registration carriers, respectively, in the first realizations of the measurement systems. The applied, manual data processing with the use of measuring microscopes was extremely laborious and did not make it possible to obtain the amount and quality of information necessary to solve the physical problems.

The development of electronics and digital and computational techniques in the last two decades have led to significant progress in image registration and processing: today, powerful pulse lasers are used as light sources, digital cameras with high resolution are used as registration devices, and the instantaneous velocity fields are calculated with modern correlation algorithms.

Although the basics of the described diagnostic method were most intensely developed in the Soviet Union, the first commercial designs of the particle-image velocimetry (PIV, the internationally accepted name of such measurement systems) appeared abroad in the late 1980s for well-known reasons. R.J. Adrian laid the foundation for the development of PIV systems (e.g., [18]). For the most detailed description of the PIV method, see the monograph in [19].

The capabilities of various modifications of the PIV method (Stereo PIV, Tomo PIV [20, 21]) for the study of the fine structure of single-phase and two-phase flows were reliably demonstrated in a number of studies [22–26] carried out by researchers of the Institute of Thermophysics of the Siberian Branch of the Russian Academy of Sciences.

Detailed studies of the characteristics of the motion of the disperse phase (solid particles) in a turbulent air flow in a tube and their inverse influence on the parameters of the carrier phase were conducted with the LDA at the Joint Institute for High Temperatures of the Russian Academy of Sciences [27–33].

Among the many other methods and means of the diagnostics of two-phase flows, we must note the

shadowgraph method, which is widely used for the visualization and subsequent measurement of the sizes and concentration of bubbles (droplets or particles), and planar laser-induced fluorescence (PLIF) is used to measure the temperature fields [34, 35].

3. TWO-PHASE FLOWS WITH PARTICLES

This section describes some results of the research on (i) the heat shield of high-speed aircrafts subject to the action of dust-laden flows, (ii) numerical simulation of the gas-dynamic interaction of an individual high-inertia particle with the shock layer of a streamlined body, (iii) the electrostatic charging of particles, which are the combustion products of the hydrocarbon fuel or are generated due to erosive destruction of the path structure of reaction engines, (iv) the combustion and propagation of detonation waves in multiphase flows, (v) the problems of the elimination of human-made airborne fine particles by acoustic waves, and others.

The destruction of the heat shield in the flight of hypersonic aircrafts (HA) in dense layers of the atmosphere (including the dust-laden layer) is determined by a complex of extreme thermal-gas-dynamic and heat factors acting on the heat shield [36–40]. As a result of such action, several internal processes develop in the volume of the heat shield; they appear as a reaction to these influencing factors. Intensive erosive destruction of the surface layer of the heat shield is a restrictive circumstance for further HA development (Fig. 3). When the heat shield is destructed, the particles are transferred from the HA surface, which complicates the simulation processes.

The results of an experimental study of the destruction of carbon heat shield materials (polygraphites and carbon composites) with allowance for their surface roughness when streamlined by a supersonic high-temperature air flow were described in [41]. The peculiarities of the gas dynamics on the rough surface of carbon–carbon composites were analyzed (the loss in the stability of the laminar flow and the generation of vortex zones). It was shown that the generation of bulges and depressions on the surface of carbon heat-shield materials as a result of aerodynamic heating significantly changes the structure of the boundary layer.

Among the works of recent years on the improvement of heat-protection materials, there are a number that should be noted [42–46]. Analysis and generalization of the results of theoretical and experimental studies of the behavior of a heat shield made from resin-like materials (highly filled elastomers) containing powder and fiber admixtures were performed in [42]. The peculiarities of the destruction of resin-like heat-protection materials under the layer of condensed phase were studied in [43]. A method to refine the depth of thermal destruction of a heat-protection coating with allowance for additional carbonization and thermal expansion of the residual coating thickness was proposed in this paper. The resistance of silicon-carbide materials to high-speed flow conditions was studied in [44, 45]. The three-dimensional problem of the coupled heat and mass exchange at the motion of a spherically blunted cone along a prescribed trajectory under different angles of attack was solved in [46]. The selection of the type of heat-protection materials, including high heat-conducting carbon materials, traditional carbon plastic coatings, and prospective, indestructible ceramic materials that allow conservation of the original geometry of the body, was analyzed.

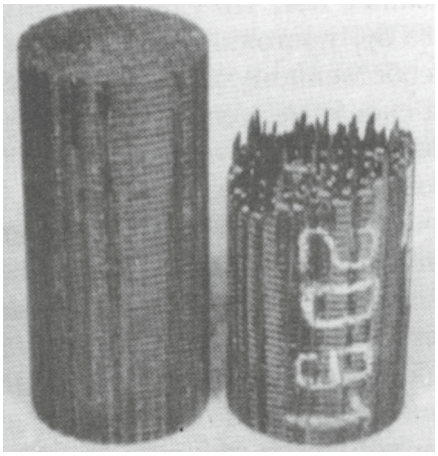

Fig. 3. Sample of a carbon–carbon composite before and after tests in a supersonic flow [38].

In addition to the direct (shock) action of particles on the streamlined surface, effects related to the influence of particles on the flow in the shock layer and on the intensity of heat transfer appear to be significant in many cases. Among these effects, the radiation heat transfer between the disperse phase and the streamlined surface is of note. In [47, 48] it was established that this effect is mostly pronounced when the particles in the flow block their own heat radiation of the heated surface, which may lead to a considerable increase in the wall temperature.

The ability to intensify the heat transfer between the two-phase flow and the streamlined body is an important factor. We point out that the mechanisms of this action and its value depend to a great extent on particle size. The intense braking and heating in the shock layer are characteristic of fine (low-inertia) particles. Upon their deposition on a surface at low velocities, the appearance of particles leads to an increase in the convective component of the heat flux. For moderately sized particles, the shock component of the heat flux plays a crucial role due to the transfer of kinetic energy upon inelastic collisions with the surface. The hardest questions arise due to the intensification of the heat transfer with flows around bodies by two-phase flows with large particles, which hardly decelerate in the shock layer. The results of numerical

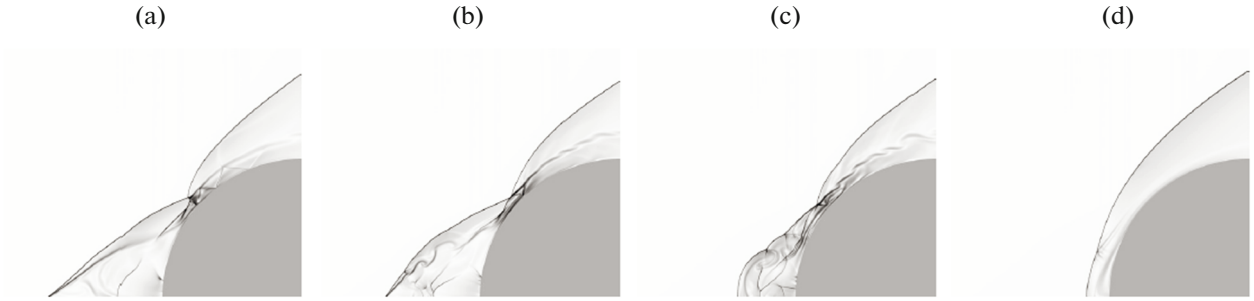

Fig. 4. Schlieren patterns of flow at different time instances [49]: (a) $\tau = 2.88 \times 10^{-4}$ s, (b) 7.54×10^{-4} s, (c) 8.68×10^{-4} s, and (d) 1.1×10^{-3} s.

modeling of the gas-dynamic interaction of an individual high-inertia particle with the shock wave are presented in [49, 50]. The evolution of the shock-wave and vorticity flows arising upon the transition of the particle reflected from the streamlined surface through the leading shock wave (Fig. 4) were analyzed in detail. It was revealed that the toroidal vortex, the flow around which causes detachment of the near-axial incident flow, plays an important role in the formation of the wave structure, which creates the conditions for intensification of the convective heat transfer.

In another important problem, the beginning of the destruction of the gas-dynamic path of the rocket engine is preceded by the appearance of combustion products in the form of multiple microparticles in the gas flow [51]. It was established that they possess an electric charge, generate an electric field, and can be registered. The currently available results laid the foundation for the contactless, electrostatic diagnostics of engines. However, the performed studies were limited by low temperatures of the gas flow (~1200 K). The use of the available data for high temperatures in the combustion chamber (2500–3500 K) may be incorrect, because the thermionic emission from the surface of condensed particles, which are combustion products of hydrocarbon fuel or are generated due to erosive destruction of the structural elements of the flow path, were disregarded. In [52] a mathematical model was constructed, and the electric and physical characteristics of combustion products in the path of the liquid-propellant rocket engine were calculated with allowance for the electric charge, and solid metal particles formed as a result of the burning of the engine structural elements. The trajectories of the metal particles, together with the velocities, temperatures, and total electric charge collected by particles due to their interaction with electrons in the combustion products, were obtained. In particular, it was established that metal particles with diameters of $d_p = 20 - 100$ μm gain an electric charge of $q_p \approx 10^{-14}$ K in a high-enthalpy flow.

The study of features of the motion of disperse phase (droplets, particles, fragments) in tornado-like vortices is of great interest for several reasons. First, the presence of disperse phase visualizes the atmospheric vortices [53–57]. Second, the measurement of the velocity of airborne disperse inclusions makes it possible to obtain the necessary information about the dynamics (velocity fields) of the air vortex [58]. Third, the hidden heat of phase transformations (primarily, condensation and evaporation) upon the generation (and disappearance) of droplets has a significant effect on the generation, dynamics, and stability of tornado-like vortices [59]. Fourth, the disperse phase may considerably influence the characteristics of the atmospheric vortex and its behavior (until its dissociation) [60–63]. Fifth, the presence of fragments and other disperse inclusions may make a large contribution to the negative consequences (damage and casualties) of the tornado.

The problems of the generation and propagation of combustion and detonation waves in multiphase media [64–67] consisting of fuel and gaseous oxidizer particles are of great interest to researchers (see also Sect. 4). Of special interest are problems of the combustion and detonation of air mixtures with hydrocarbons [68, 69] and metal particles (aluminum, magnesium, and boron). The processes of the combustion of hydrocarbons and metalized fuels have both many common laws and a series of principal differences [70]. The combustion of droplets of hydrocarbon fuel occurs in the gas phase, because it is the evaporation products that are burning. Here, the temperature of the droplets themselves is considerably lower than the temperature of the combustion products. The combustion of metallic particles is accompanied by surface and gas-phase chemical reactions and the generation of condensed products on the particle surface and in the combustion products. In addition, the temperature of particles can exceed the temperature of surrounding gases.

A physico-mathematical model that allows the description of the processes of the self-combustion, combustion, and denotation of combustible metal-gas mixtures (suspensions of aluminum, magnesium, and boron) was developed in [71]. The disperse particles were assumed to be multicomponent, and the pro-

cesses of the heating, melting, and evaporation of the particle material were taken into account, along with the surface reactions, in which both liquid and gas components take part. The influence of the mass flow rate of metal particles on the minimum velocity of the stationary detonation was studied. It was established that the parameters of the stationary detonation wave asymptotically tend to the equilibrium values: to a point on the equilibrium detonation adiabatic curve.

The problem of the elimination of human-made airborne fine particles is topical. Such particles are formed upon the combustion or fragmentation of solid bodies and the processing of various raw materials and metals and in processes of acid and caustic etching [72–74]. Modern cleaning devices cannot collect micron-sized disperse particles. The action of the acoustic wave in bounded volumes near the resonance frequencies promotes not only the intensification of particle sedimentation on walls but also their enlargement due to collisions between each other [75–77].

The characteristics of the reflection and refraction of an acoustic wave passing through the boundary of two multifractional gas suspensions at a right angle were studied in [75]. The dependences of the absolute values of the reflection and refraction coefficients on the frequency $\omega\tau_p$ (ω is the frequency of excitation, and τ_p is the dynamic relaxation time of particles) were obtained for different particle mass concentrations. It was shown that, if the same gas is used as a carrier medium, then there is a monotonic dependence of these coefficients on the particle mass concentration in two cases: (i) when an acoustic wave is incident on the interface between a pure gas and a multifractional gas suspension and (ii) when an acoustic wave is incident on the interface between a monodisperse mixture of gas and solid particles and a multifractional gas suspension. If gases with different thermophysical properties are used as carrier media, then the monotonic character of the reflection and refraction coefficients on the mass concentration is lost.

The propagation of sound in a multifractional gas suspension with polydisperse inclusions was studied in [76]. Sand particles (d_p = 50–100 μm), aluminum particles (d_p = 5–10 μm), and water droplets (d_d = 500–1000 μm) were considered fractions. The mass concentration of all three fractions was the same (M = 0.3). It was revealed that the presence of three fractions with different inclusion sizes lead to three characteristic inflections that depend on the relative speed of sound on the dimensionless excitation frequency. The three identified local maxima depend on the decay decrement in the wavelength σ on the dimensionless frequency (Fig. 5) and are related to the difference radii and thermophysical properties of inclusions of different fractions.

The propagation of planar, spherical, and cylindrical waves in multifractional gas mixtures with polydisperse inclusions was studied in [77]. A closed system of equations for these mixtures was constructed, and the unified disperse relation was derived. The presence of different thermophysical properties, inclusion size, and inclusion-size distributions were taken into account in the calculations. The evolutions of the pulse-pressure perturbation in the considered mixtures were calculated. It was shown that accounting for the presence of fractions in the mixture and for the heat transfer leads to stronger wave decay.

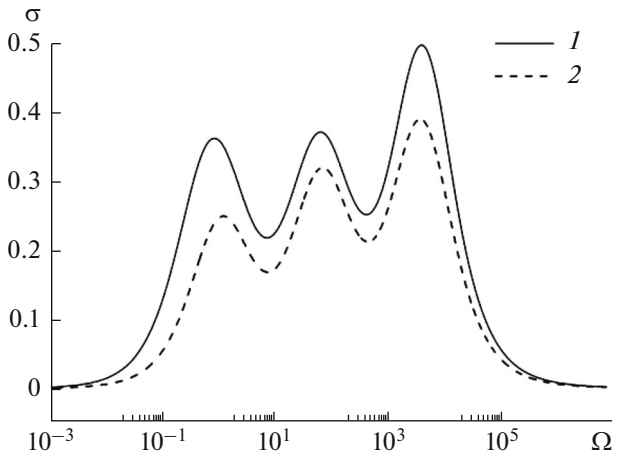

Fig. 5. Decrement of decay over the frequency of dimensionless excitation with (*1*) and without (*2*) allowance for the heat transfer [76].

Many technological processes in the chemical, petrochemical, food, and other industries require a high degree of purification of highly viscous media in order to obtain a quality product, to reduce equipment wear, and to prevent incidents. Devices with dual actions are used to separate such media. They combine filtering, which provides the required degree of purification, and cleaning in the force fields, which reduces energy consumption and increases the service life of equipment. The dependence of the separation efficiency of solid particles and the stability of the spiral motion of a viscous liquid in a converging channel with an internal, rotating, permeable, cylindrical partition were numerically studied in [78]. Analysis of the results showed that vortices can arise in the converging flow and can negatively affect particle separation.

Metallic disperse powders are widely used in practice. One commonly used method to obtain metallic powders is based on the evaporation of a metal or alloy with subsequent condensation and solidification [79]. There are a significant number of works on the condensation of metallic nanoparticles. Experimental data on the functions of the nanoparticle-size distribution showed that they differ from the classical ideas of atom attachment to the cluster [80] and that coagulation is observed also on some stages of condensation due to the collisions of small particles [81]. For an

accurate model of the coagulation, it is necessary to determine the collision frequency between the clusters. This requires knowledge of the velocities, concentrations, and values of interaction [82].

A molecular-dynamic (MD) study of the dependence of the radii of small metallic clusters in the process of copper gas-phase condensation on the number of atoms in them was performed in [83]. The frequency of collisions between clusters was determined with formulas of molecular-kinetic theory. It was established that the dependence of cluster radii on the particle number has a form close to the classical one ($r_c \sim n^{1/3}$); however, the mean cluster radius appears to be approximately 40% larger than the radii for a cluster that is considered to be a droplet of massive liquid.

The results of an MD simulation of the condensation of metallic vapors (Cu or Ti) in an inert gas medium, argon (Ar), were statistically analyzed in [84]. Condensation occurs with the generation of small particles consisting of metallic atoms. The internal energy was used as a key characteristic that allows the prediction of the cluster life span, from its generation to dissociation (i.e., the ability of a cluster to grow). The internal energy includes the kinetic energy of atoms in the system of the cluster center of mass and their potential energy. It was shown that, in addition to the traditional evolution of clusters in the size space, the evolution of clusters in the energy space must also be considered.

4. TWO-PHASE FLOWS WITH DROPLETS

This section describes some results of research on (i) the efficiency of water injection into gas-turbine power units, (ii) the dynamics of liquid fragments (droplets, films, and streamlets) moving over a rigid body, (iii) the separation of gas–droplet flows, (iv) the effect of water injection on the structure of a detonation wave, (v) the acoustic coagulation of aerosols, (vi) the generation of liquid particles upon metal ablation, (vi) the surface tension of vapor–liquid interfaces, and (vii) the ability to separate stable water–oil emulsions.

The organization of efficient water injection into gas-turbine power units, which work according to different steam–gas cycles, requires the study of the combined action of various mechanisms on the motion of droplets and their sedimentation on the path elements. Wet compression refers to a reduction in the temperature of the compressed air as a result of the evaporation of water droplets injected into the air flow. Because the specific rate of evaporation (per unit volume) of the disperse phase is in inverse proportion to the square of the droplet size, the efficiency of the wet compression becomes maximal in the case of a highly dispersed injection of the overheated water.

Note that the process of droplet sedimentation has a crucial effect on blade erosion, which occurs with the long (up to 20000 h) operation of a gas-turbine power unit with water injection and leads to a reduction in the operation characteristics.

The results of experimental studies of the characteristics of a gas–droplet jet spray and disperse-phase sedimentation on the surface of the streamlined profiles were described in [85–87]. The angle of attack of blade profiles, the degree of water overheating before the jet nozzle (which determines the size of the obtained droplets), and the droplet concentration were varied in the experiments. A correct accounting for the two main mechanisms of sedimentation (inertial and turbophoretic ones) based on well-known techniques made it possible to obtain satisfactory agreement with the experimental data for the rate of droplet sedimentation and the thicknesses of the water films generated on surfaces streamlined by the two-phase flow.

The original studies of pulse sprays were performed in [88, 89]. It was convincingly demonstrated that a significant improvement in cooling efficiency is possible when the pulse spraying is organized, which opens great prospects for its use in several practical applications.

The dynamics of liquid fragments (droplets, film, or streamlets) moving over a rigid body has been studied in recent decades with respect to problems of power engineering, the food and chemical industries, and flight safety [90–92]. The case of droplets occurring on a vertical or inclined planes in a motionless gas has been sufficiently studied. However, at high speeds (typical of aviation), the study of droplet dynamics is complicated due to the presence of a boundary layer, the thickness of which is comparable with the droplet size and varies along the flow. Note that this boundary layer is rich in three-dimensional and nonstationary structures. The study of the hydrothermodynamics of a droplet with allowance for its cooling to the freezing temperature or below is necessary in order to predict correctly the region of the appearance of barrier ice, which poses a serious threat for aircraft [93].

Experiments were performed in [94] on the example of a model profile of a rectangular wing. The limiting hysteresis of the contact angle with respect to the surface properties was measured by the inclined-plane method. A physico-mathematical model of the droplet dynamics on a flat surface in a gas flow was also developed. The forces attracting the droplet, along with the adhesion force and the dissipative force of internal friction, were taken into account in the equation of droplet motion. The flow velocity at the beginning of droplet motion was determined. Important dependences of the droplet velocity on its characteristic size and air velocity were revealed. The experimental-theoretical algorithm developed in the work can be used to conduct experiments on a considerably wider range of governing parameters (the droplet size, the surface tension coefficient of the liquid, the gas flow velocity, and the limiting contact angle).

Single-phase swirled (vortex) flows are characterized by large local gradients of averaged and pulsation velocities, which are determined by complex hydrodynamic phenomena due to the action of the centripetal force, the radial pressure gradient, and the Coriolis force [95–97]. Vortex two-phase flows under the conditions of an abrupt pipe of channel divergence are widely used to stabilize the combustion process in industrial combustion setups and separators. The formed recirculation flow, which is caused by an abrupt divergence or constrained swirling, has a decisive effect on the intensity of heat-transfer processes and the propagation of disperse phase.

Numerical simulation of the swirl parameter on the heat transfer in a gas–droplet flow behind an abrupt pipe divergence was carried out in [98] on the basis of a Eulerian approach with a system of 3D RANS equations. It was shown that, without swirling, there is a rapid dispersion of droplets over the pipe cross-section behind the abrupt pipe divergence. In the case of swirling, an increase in the concentration of small particles was observed on the axis of the pipe due to their collection in the zone of inverse currents due to the turbophoretic force. It was found that large particles are positioned in the near-wall region of the channel due to the centripetal forces. The calculations showed that a significant (two-fold) reduction in the length of the separated-flow region occurs in the swirled flow. The appearance of particles in the flow led to a considerable increase in heat emission (by more than 2.5 times) in comparison with the single-phase swirled flow (Fig. 6).

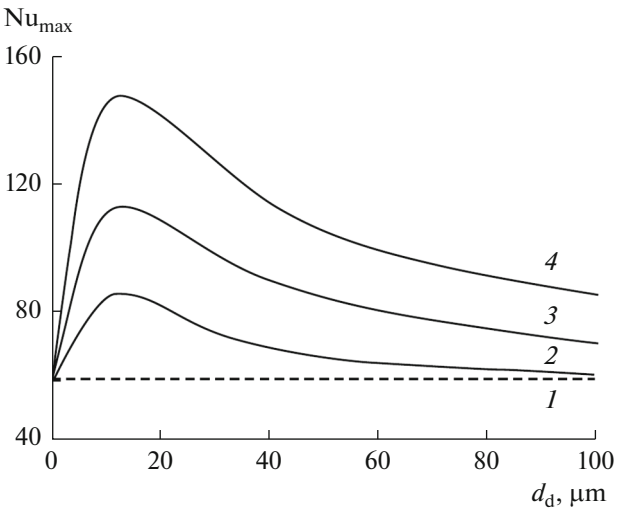

Fig. 6. Effect of the introduction of evaporating droplets on the maximum value of the Nusselt number in a swirled, two-phase flow at a swirling parameter of $S = 0.5$ [98]: (*1*) single-phase flow; the initial mass concentration of droplets: (*2*) 0.02, (*3*) 0.05, (*4*) 0.1.

The problems of the generation and propagation of combustion and detonation waves in multiphase media attract strong interest from researchers (see also Sect. 3). Of special topicality is the suppression of the detonation and deflagration with the water droplets sprayed in the zone of the propagation of detonation waves in inflammable gas mixtures. The main results of the study of the combustion and detonation of gas and gas–droplet mixtures were given in well-known monographs [99–102].

The effect of water spraying on the detonation-wave structure was numerically studied, and the conditions of the existence of the Chapman–Jouguet detonation regime in an inflammable gas–droplet mixture were studied in [103]. The effect of water spraying on the structure and minimal propagation speed of a stationary detonation wave was determined. The values of the mass concentration and initial diameter of the water droplets that lead to the decay of detonation in an inflammable hydrogen–air mixture were found.

The nonlinear effects that appear with acoustic oscillations in inhomogeneous media attract great attention due to their prospects for practical application. Of special interest is acoustic coagulation, which may be used in the sedimentation of aerosols in industrial wastes (e.g., water vapor in wet cooling towers and other liquids in thermal engineering facilities) or in the purification of liquids in the food and chemical industries. The study of the propagation of acoustic waves in aerosols is complicated due to the need to take into account the multiphase and polydisperse character of the aerosols and the transient and nonequilibrium character of the processes of interphase interaction [104–107].

The aerosol dynamics was experimentally studied in [104] in an open pipe under the action of acoustic waves of different intensities near the first eigenfrequency in transient mode (where shock waves are not generated). It was found that the shape of the aerosol pressure-wave distributions in time becomes somewhat different from the harmonic shape only with resonance. The time of aerosol clearing was determined for various frequencies and amplitudes of piston displacement. The minimal time of aerosol clearing was revealed at the first eigenfrequency. It was concluded that the aerosol clearing in transient mode is 1.5 times faster than the clearing in shock-free wave mode at identical amplitudes of piston displacement.

In [105] a closed system of linear differential equations of motion was constructed for a multifractional mixture of gas, liquid droplets, and solid particles of different sizes and thermophysical properties. The dispersion relation governing the propagation of small-amplitude perturbations of various geometry (planar, spherical, and cylindrical) was obtained. The low- and high-frequency asymptotics of the linear coefficient of decay, along with the equilibrium and frozen speed of sound, were determined. The effect of the disperse phase parameters on the dissipation and dispersion of sonic waves was analyzed. An important conclusion

was drawn about the substantial impact of contaminants (solid particles) on the dynamics of weak waves in vapor–gas–droplet mixtures.

The effect of disperse-phase fragmentation on the development of the shock wave propagating from the pure gas into the aerosol was studied in [106].

A numerical model of the hydro- and thermodynamics of a polydisperse vapor–droplet mixture in a coaxial cylindrical channel was constructed in [107]; this model takes into account the processes of droplet evaporation, coagulation, and fragmentation and the condensation of vapor with the presence of speed and temperature phase slips. Interesting conclusions were made: (i) the large concentration of the donor fraction that is generated upon vapor condensation leads to intensification of the coagulation process and to rapid droplet growth for all fractions that are nonequilibrium in their velocity; (ii) the further growth of droplets of different fractions implies the appearance of flow regimes with the achievement of the critical Weber number and replacement of the coagulation process with the process of their fragmentation; (iii) as a result of competition between coagulation and fragmentation, there is a restructuring near the critical Weber number from a polydisperse, multispeed mixture to a two-speed mixture with two predominant droplet sizes. As an example, the flow of a vapor–droplet mixture in a coaxial channel of the heat-absorbing element of the heater-regasifier of a liquefied natural gas was calculated in [107].

The generation of liquid droplets occurs in the processes of metal ablation. Under the action of femtosecond laser pulses with a moderate intensity of 10^{12}–10^{13} W/cm^2 on metals, conduction electrons are isochorically heated with the subsequent transfer of energy to the lattice by the electron–phonon heat transfer and its rapid melting (during 10^{-12}–10^{-11} s). The surface nanolayer is removed by powerful tension stresses due to isochoric heating. Two ablation modes are distinguished: spalling and fragmentation ablation.

The first mode of metal destruction is caused by the cavitation process of the formation and growth of the vapor phase in the melt in the expansion wave and by the ablation of part of the melt in the form of a thin spallation plate in the liquid phase. After solidification of the melt, cell nanostructures are generated on the surface of the metal.

Fragmentation ablation arises at higher intensities and is associated with the explosive removal of a substance at the hydrodynamic expansion of a supercritical fluid in the form of a vapor–droplet mixture.

Studies of the femtosecond-laser ablation of tantalum were performed in [108] with optical interference microscopy. It was discovered that the depth of the spallation crater is approximately three times larger than the depth of the fragmentation crater. Studies of the flame structure revealed the ejection of the substance in the form of a condensed layer with spallation ablation and in the form of a vapor–droplet mixture with fragmentation ablation.

Similar studies on the ablation of a titanium target with a single action of laser pulses with a duration of 40 fs were carried out in work [109]. The results of the study of the morphology and nanorelief of crater surfaces demonstrate the spallation character of destruction of the metal surface layer in the condensed state.

A comparison of the thermomechanical ablation of the metals gold and nickel, which are considerably different in their thermophysical properties, is presented in [110]. The variation of the target reflectivity with respect to the energy density of the femtosecond laser pulse was studied. The values of the ablation threshold in the absorbed energy density were determined; they were 0.14 and 0.11 J/cm^2 for gold and nickel, respectively.

The value of the surface tension of multicomponent droplets is of great importance for many physicochemical processes. The studies in the domain of thermodynamics of microheterogeneous systems done in the 1950s clearly showed the error in the equalization of the properties of the new phase nucleus and the macroscopic phase [111] and the need to transition to kinetic methods to describe the formation of droplets with different numbers of components [112].

A molecular theory based on the lattice gas model was used in [113] to describe the surface tension of the vapor–liquid interfaces of single- and two-component simple liquids. The calculation of the mixture surface tension was carried out in the quasi-chemical approximation of the allowance for the intermolecular interactions of the nearest neighbors. The model parameters previously obtained from experimental data on the volume surface tensions made it possible to calculate the surface tensions of the vapor–liquid interfaces of single- and two-component droplets of different sizes as a function of their radii. The minimal size of thermodynamically stable small droplets with the properties of a homogeneous phase inside them was estimated.

The separation of stable water–oil emulsions is one of the most important problems of the oil industry. Highly viscous oil forms strong shielding envelopes around water droplets, and the destruction of such systems is complicated. This characteristic leads to the fact that the sedimentation and merging of water–oil emulsions is difficult, even in the field of centripetal forces. The action of the electromagnetic field is an efficient means of heating of rheologically complex fluids. The heating intensity and the destruction dynamics of emulsions depend on the physical parameters of the system and the characteristics of the applied field. The application of microwave fields to separate stable water–oil emulsions is one of the most promising technologies. The conducted experiments showed both a positive effect [114–117] from the impact of microwave radiation on water–oil emulsion

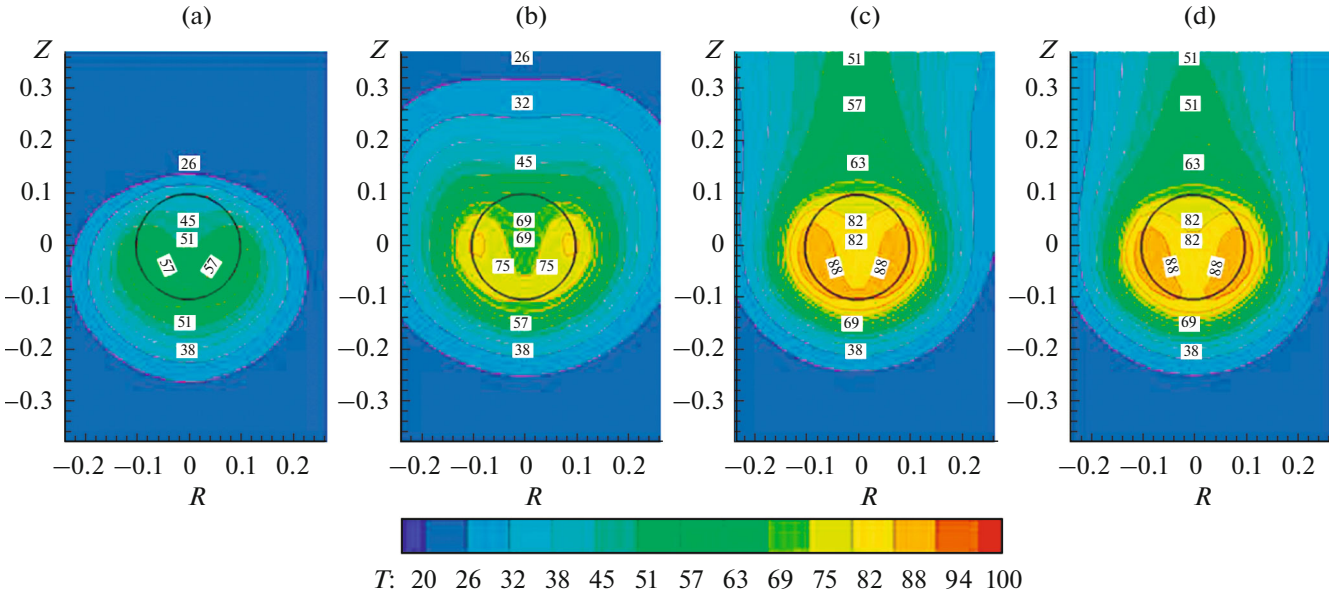

Fig. 7. Temperature field in droplet and surrounding liquid with microwave heating at different time instances [120]: (a) 5 s, (b) 15 s, (c) 25 s, and (d) 35 s.

(merging of water globules and separation of emulsion) and the possible negative effects [118, 119] (droplet breaking and the generation of a smaller, finely dispersed phase).

The heating of an emulsion droplet of the water-in-oil type via electromagnetic microwave radiation in the gravity field was numerically simulated in [120] with allowance for the temperature dependence of the viscosity of liquid surrounding a droplet (Fig. 7). The considered system of equations of heat convection in the well-known Boussinesq approximation was solved with the VOF method. It was revealed that droplet heating occurs mostly near its surface due to appearing convective structures, which is a factor that promotes the local heating of the shielding envelope and the generation of the finely dispersed phase. The entire electromagnetic microwave action on an emulsion droplet may be divided into three subsequent stages: the static stage (Figs. 7a, 7b), the dynamic stage (Fig. 7c), and the quasi-stationary stage (Fig. 7d). It was found that there is an optimal range of microwave-field power that leads to an intensive deposition of water droplets and the destruction of the water–oil emulsion.

5. TWO-PHASE FLOWS WITH BUBBLES

This section describes some results of research on (i) the characteristics of the boiling process for water underheated below the saturation temperature, (ii) the local heat transfer in the vicinity of the contact line under vapor bubbles upon the boiling of liquids, (iii) the generation of a porous layer of nanoparticles upon the boiling of a nanoliquid, (iv) the structure of the separation of a turbulent bubbly flow and the flow in the bubble impact jet, (v) the characteristics of the reflection and propagation of acoustic waves at the boundary of pure and bubbly liquids, (vi) the detonation waves in the bubbly media, (vii) the efficiency of the bubbly method for water purification, etc.

The generation of bubbles in an originally one-phase liquid occurs in the boiling process. The boiling of a subcooled liquid is widely used in technological processes associated with the removal of higher heat fluxes, including extreme ones. Such surface boiling is used in rocket-space technology, beam technology, metallurgy, and pulse-magnetohydrodynamic facilities. The realized heat-transfer coefficients for water can reach hundreds of kW/(m^{2}K) and can considerably exceed the similar characteristics achieved with other methods of heat transfer. The recorded density of heat fluxes at the subcooled water is 276 MW/m^2 [121].

It is worth noting that, at boiling of subcooled water, we talk about the boiling of degasified (deaerated) liquid. In the opposite case, release of a large amount of gas dissolved in it and its collection in some spatial regions at increasing temperature (at reduction in water underheating) may lead to emergency situations [122] (Fig. 8).

One well-known method to intensify the boiling process of a saturated liquid is surface modification with micro- and nanostructures of various types [123]. This leads to an increase in the heat-exchange surface and the number of active vaporization centers, improved operational stability of the acting centers, a change in bubble size and the frequency of bubble generation, and the stimulation of bubble evacuation from the heating surface.

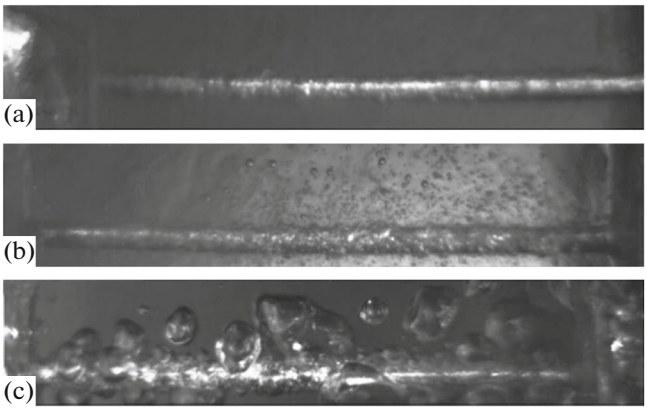

Fig. 8. Video frames of water boiling in a large volume on a capillary, $d_d = 1$ mm [122]: (a) degasified water, (b) non-degasified water, and (c) water saturated with carbon dioxide.

Experimental data on the boiling of subcooled water under the constrained flow conditions on a surface formed via microarc oxidation and the sedimentation of Al_2O_3 nanoparticles from a boiling nanoliquid are presented in [124]. A large underheating of the boiling liquid and its deep deaeration fully deactivates the acting vaporization centers after condensation (collapse of a vapor bubble). Figure 9 shows the video frames of the last stage of such a collapse. It is clearly seen that this takes place not only above and from the lateral surface; it also captures the region at the bottom part of the bubble. After the bubble collapse, there is no remaining vapor phase nor air bubble, which serve as nuclei of the new vapor phase in the case of developed boiling of a saturated liquid, on the heating surface. It was revealed that a large underheating of the liquid (30–76°C) and a high wettability of the structured surface cause intensive deactivation and lead to a chaotic distribution of vaporization centers in time. The characteristic size of vapor bubbles was approximately 200–250 μm, and the life time of the bubbles was 200–500 μs. The use of the coating generated with microarc oxidation increased heat transfer by 20–30%.

The mode of bubbly liquid boiling is one of the most efficient means of heat removal. High-speed thermographic macro filming, which made it possible to study the dynamics of the distribution of the heater temperature field under separate vapor bubbles at a high spatial resolution with the boiling of ethanol and water, was first carried out In [125]. It was shown that the density of the heat flux removed from the surface upon the evaporation of the microlayer can be significantly larger (by 15–20 times) than the density of the heat flux averaged over the heat-release surface.

Objectively, the film boiling of a saturated (or weakly subcooled) liquid is one of the simplest ways to study the boiling modes. The temperature of the heated surface in this mode exceeds the limit superheating temperature of the liquid, which excludes the possibility of its direct contact with the wall. Hence, the heat transfer is determined by the heat conduction via the vapor film, which is responsible for its low intensity.

The results of an experimental study of the heat-exchange modes upon the water cooling of steel balls with a technically smooth and modified surface (finely dispersed carbon coating) heated to a high temperature was presented in [126]. It was discovered that the mode of intense heat transfer with film boiling at surface heat fluxes of 6 MW/m^2 occurs upon the cooling of both samples in subcooled water. The presence of a carbon coating leads to intensification of the heat transfer and a reduction in cooling time.

A model of the generation of a porous layer of nanoparticles (nanolayer) on the heater surface during the boiling of a nanoliquid was developed in [127]. One peculiar property of nanoliquids is their ability to

Fig. 9. Collapse of a vapor bubble (lateral view) [124]. Time interval between frames, 100 μs; heat-flux density, 1.5 MW/m^2; underheating value, 76°C. The water is still, and the surface is an aluminum plate with Al_2O_3 coating.

increase significantly (by two or more times) the value of the critical heat flux at negligible concentrations (0.001–0.1 vol %). Figure 10 presents images of the nanolayer surface obtained with a scanning electron microscope after experiments on boiling with nanoliquids based on water with ZrO_2 particles with an average size of approximately 100 nm. Modification of the heating surface in power-engineering equipment with the generation of a porous layer on it is more advantageous than the use of a nanoliquid as a heat-conducting substance. The study of nanolayer generation upon boiling will make it possible to gain an understanding of its properties and the effect on heat transfer upon boiling, as well as the boiling crisis.

Bubbly flows are widely used in chemical technology, power engineering, and other areas of engineering. As a rule, they are turbulent and have a considerable interphase interaction between the liquid and bubbles. They may become more complex with flow separation at sharp edges, polydispersity, the fragmentation and coalescence of bubbles, and interphase heat transfer. It is well known [128, 129] that the recirculation flow generated upon flow separation at a sharp edge to a large extent determines the structure of the turbulent flow and affects the intensity of the processes of momentum, mass, and heat transfer. Correct modeling of the bubble distribution over the channel cross section is of great importance for the safe operation and prediction of various scenarios of emergency situations in heat generators of thermal and nuclear power stations.

The results of numerical simulation of the structure of a polydisperse, non-isothermal, bubbly, turbulent flow and the heat transfer behind an abrupt pipe divergence with allowance for the processes of fragmentation and coalescence were provided in [130]. The developed mathematical model is based on the Eulerian description with allowance for the inverse effect of bubbles on the averaged and fluctuating characteristics of the carrier phase. The turbulence of the carrier phase was calculated with the transfer equations of Reynolds stresses. The bubble dynamics was described with allowance for the variation in the average volume of bubbles due to expansion upon variation in the density, fragmentation, and coalescence. The calculations were carried out at different initial air-bubble diameters in the range $d_{b0} = 1$–3 mm and with volume gas contents of $\beta = 0$–10%. It was established that small bubbles occur over practically the entire cross section of the pipe, whereas the large ones pass mostly through the flow core and the shear mixing layer. The bubbles behind the separation section have a smaller size than the initial bubbles due to the fragmentation at an increase in the intensity of the turbulence in the separation flow. The increase in the size of the disperse phase causes an increase in the turbulent fluctuations in the liquid phase upon separation flow around the large bubbles. It was demonstrated that the introduction of air bubbles leads to a considerable decrease in the length of the separation zone (up to 1.5 times) and an increase in the heat-transfer intensity (up to two times); both of these effects become stronger as the bubble size and concentration increases.

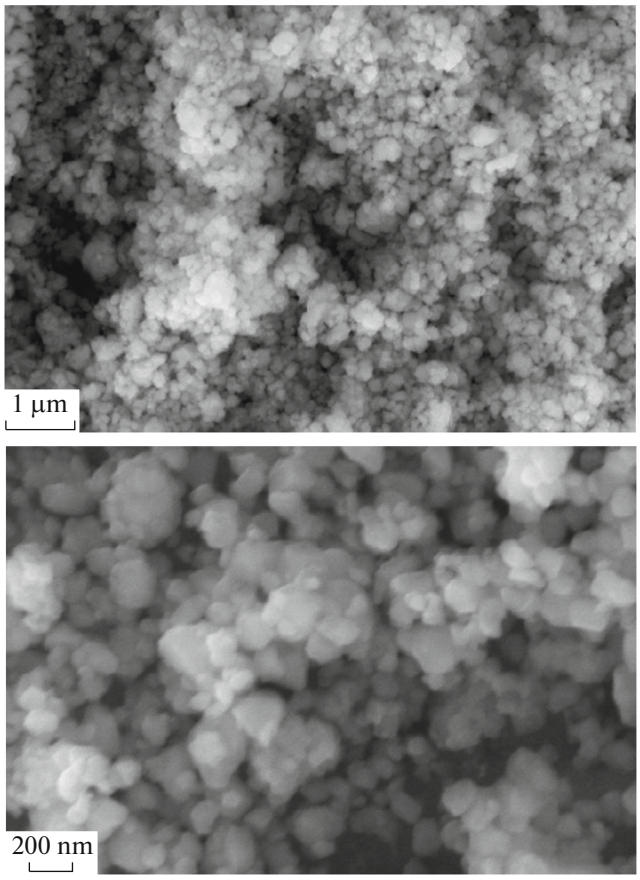

Fig. 10. Grains (nanoparticles) composing the surface coating after boiling of the nanoliquid [127].

The heat transfer in a submerged, bubbly, impact, pulse, circular jet was numerically modelled in [131]. The effect of the variation in the pulse frequency and the volume gas content on the heat transfer in a gas–liquid impact jet was studied. The imposition of pulses on an impact, bubbly jet causes both suppression of the heat transfer in the vicinity of the braking point (up to 20–25%) in the region of low frequencies and its intensification (up to 15–20%) as compared to a stationary, impact, bubbly jet with the same time-averaged mass flow rate of the two-phase jet.

A layer in which very long-distance sound propagation is possible can appear in sea water at some depths due to a decrease in its density or the speed of sound for different reasons. This layer is called the underwater sound channel. The layer with the minimal speed of sound usually appears at a depth of several hundreds of meters. Above this layer the speed of sound increases due to the increase in water tempera-

ture; below this layer, it increases due to the increase in pressure. The described phenomenon was independently discovered by the American scientists J.L. Woezel and M. Ewing [132] and the Soviet scientists L.M. Brekhovskikh and L. D. Rozenberg [133, 134]. Underwater sound channels may appear due to variation in the water salinity, the presence of nanobubbles, the vital activity of microorganisms, the migration of bubbles from the bottom, etc.

The propagation of a wave pulse in liquid containing bubbles was considered in [135]. The criteria for wave-pulse suppression by the bubbly screen were established with respect to the initial system parameters. It was demonstrated that a bubbly layer with a sufficiently moderate initial volume content of bubbles can totally suppress the wave signal.

The characteristics of the reflection and retraction of harmonic waves at the interface between pure liquid and liquid with bubbles with vapor–gas mixture were studied in [136, 137] at their normal [136] and inclined [137] incidence. The effect of variation in the equilibrium temperature in the range of 300–373 K (boiling point) was numerically analyzed for two initial bubble sizes: $d_b = 10^{-6}$ and 10^{-3} m. The mass vapor content in bubbles varied in the ranges $k_0 = 0.023$–0.996 and $k_0 = 0.001$–0.347 for coarsely and finely dispersed systems, respectively. The influence of the excitation frequencies on the reflection coefficient and the refraction index of sound was studied. It was shown that, when the wave is incident from the side of bubbly liquid on the boundary at a certain band of frequencies higher than ω_b (ω_b is the eigenfrequency of bubbles), the condition of the total internal reflection can be realized.

The dynamics of weak harmonic perturbations in a superheated, water–air, bubbly medium was studied in [138]; in addition to the water vapor, there was an inert gas that did not participate in the phase transitions in the bubbles. A detailed analysis was carried out for the patterns of the stability zones of the considered systems with respect to the degree of liquid superheating on the plane of the volume content–radius of the bubbles with an increase in the equilibrium pressure from 0.1 to 10 MPa. The effect of the initial superheating (from hundredths to one degree) and the effect of the pressure increase on the dispersion of harmonic waves, along with the dependence of the increment on bubble radius for instable systems, were established.

The collapse of a spherical cavity in an incompressible liquid was first studied by Rayleigh in 1917 [139]. In particular, a mathematical model was developed for the calculation of the bubble radius during its compression. Ya.B. Zeldovich [140], C. Hunter [141], E.I. Zababakhin [142], K.V. Brushlinskii [143], A.N. Kraiko [144], and many others (e.g., [145, 146]) studied the problem of the collapse of a spherical cavity in compressible and incompressible liquids.

Detonation is a universal phenomenon. Detonation waves exist in various homogeneous and heterogeneous media. Note that detonation in bubbly media is a unique phenomenon, because the waves of a bubbly detonation can exist in systems with an extremely low energy content. Having attributes common for all waves (a self-maintaining, autowave, stationary process), the wave of bubbly detonation has several characteristics that are manifested in the structure, properties, and propagation mechanism [147–150].

The detonation process is a result of the collective interaction of gas bubbles uniformly distributed in a liquid. The gas bubbles ignited in the detonation wave radiate the shock waves in the surrounding liquid, and these waves compress and inflame the bubbles ahead of the detonation wave. The characteristics of detonation waves do not depend on the initiation conditions and are determined by the parameters and physicochemical properties of bubbly media [151–154]; therefore, the detonation is an autowave process.

The dynamics of detonation waves in a chemically active bubbly liquid was numerically simulated with allowance for the relative motion of phases in [155]. In this study, an acetylene–oxygen stoichiometric mixture $C_2H_2 + 2.5O_2$ is taken as a gas phase, and a mixture of glycerin and water with the volume concentration of glycerin 50% is taken as a liquid. The ignition of gas inside bubbles occurs when some critical temperature T_* is reached. As a result of an instantaneous chemical reaction, the gas temperature also changes by some value ΔT (which corresponds to the calorific value of gas), due to which the pressure in gas and liquid increases. The described process corresponds to the fact that the time of chemical reactions is significantly shorter than the characteristic time of bubble pulsations. The calculations showed that accounting for two-speed effects lead to a faster decrease in the gas temperature in bubbles and in the pressure in the liquid behind the detonation wave, practically to their initial values.

An important feature of the dynamics of vapor–gas bubbles is the ability to reach very high temperatures, densities, and pressures in them. In [156] the features of the shock compression of vapor bubbles with a diameter of 1 mm and the increase in their asphericity during collapse were compared in the hydrocarbon liquids acetone, benzene, and tetradecane. At the beginning of the compression, the vapor is in the saturation state at a pressure of 1.03 MPa, while the bubble collapse is caused by a pressure in the liquid of 5 MPa. It was established that, with the collapse of such a bubble in acetone, only weak compression waves appear in its cavity. In bubbles in benzene and tetradecane, which have a considerably larger molecular mass and a correspondingly lower speed of sound in vapor, intense, radially converging compression waves are generated, and they transform into shock waves.

The purification of water from various admixtures is a topical problem. If the contaminant molecules are not soluble in water, natural water self-purification [157] occurs upon the displacement of the admixture from the water volume to its surface. The process of the displacement of admixture molecules towards the water surface can be accelerated by the character of their interaction in water and by bringing the interface closer to them. One of the proposed methods consists of the introduction of bubbles into the water volume. In this case the bubble surface is an interface between water and air inside the bubble, and the process of the attachment of an admixture molecule to the bubble surface may be beneficial in terms of energy [158].

A method of water purification from admixture molecules with air bubbles was considered in [159] The bubbles are generated at the bottom of a vessel; floating upwards, they capture the admixture molecules and transfer them to the surface of the water flow. The admixture molecules are then removed from the surface or destroyed on it under the action of the surface electric discharge. Theoretical and experimental analyses demonstrated that this method of water purification can be realized in practice. It was concluded that this method is inappropriate for large-scale water purification due to the large number of air molecules needed to remove a single admixture molecule, but it can be convenient to remove, e.g., biohazardous admixtures, from water.

An underwater rocket launch is accompanied by processes of the intense exhaust of hot fuel-combustion products into water and intense heat and mass transfer of hot gas with liquid, which occur at the ignition of the propulsion engine in a silo submerged in water, at the start of solid-propellant gas generator in water, and in the processes concurrent to the launch [160]. As a result, there is a complex, significantly nonstationary pattern of the interaction between hot gas jets and water, which leads to the generation of a two-phase flow with bubbles. Note that the gas exhaust creates an intensive circulation of liquid, which, in turn, acts on floating bubbles and gas–liquid structures.

A physical model that allows mathematical simulation of the interphase interaction at the hot gas–water interface was developed in [16]. The thermal and gas-dynamic processes in underwater rocket launch were calculated.

CONCLUSIONS

The problems and features of the study of the flows of continua containing a disperse admixture in the form of solid particles, droplets, or bubbles were considered. Some results of recent studies of two-phase flows and the prospects for their use to solve a wide range of applied problems were described.

FUNDING

The work was supported by the Russian Foundation for Basic Research, project no. 18-08-01382.

REFERENCES

1. Varaksin, A.Yu., Romash, M.E., and Kopeitsev, V.N., *Tornado*, New York: Begell House, 2015.
2. Varaksin, A.Y., *Turbulent Particle-Laden Gas Flows*, New York: Springer, 2007.
3. Varaksin, A.Yu., *Collisions in Particle-Laden Gas Flows*, New York: Begell House, 2013.
4. Varaksin, A.Yu., *High Temp.*, 2013, vol. 51, no. 3, p. 377.
5. Zaichik, L.I. and Pershukov, V.A., *Fluid Dyn.*, 1996, vol. 31, no. 5, p. 635.
6. Pialat, X., Simonin, O., and Villedieu, P., in *Proc. ASME Fluids Eng. Summer Conf. FEDS2005-77078*, Houston, USA, 2005.
7. Zaichik, L.I., Skibin, A.P., and Solov'ev, S.L., *High Temp.*, 2004, vol. 42, no. 1, p. 111.
8. Alipchenkov, V.M. and Zaichik, L.I., *Fluid Dyn.*, 2000, vol. 35, no. 6, p. 883.
9. Buyevich, Y.A., *J. Fluid Mech.*, 1971, vol. 49, p. 489.
10. Lesieur, M. and Metais, O., *Ann. Rev. Fluid Mech.*, 1996, vol. 28, p. 45.
11. Kuerten, J.G.M. and Vreman, A.W., *Phys. Fluids*, 2005, vol. 17, 011701.
12. Peskin, C., *Acta Numer.*, 2002, vol. 11, p. 1.
13. Amsden, A.A. and Harlow, F.H., *The SMAC method: Numerical technique for calculating incompressible fluid flows*, Los Alamos Sci. Lab, 1970.
14. Belotserkovskii, O.M. and Davydov, Yu.M., *Nestatsionarnyi metod krupnykh chastits dlya resheniya zadach vneshnei aerodinamiki* (The Nonstationary Method of Large Particles to Solve External Aerodynamics Problems), Moscow: Vychislit. Tsentr Akad. Nauk SSSR, 1970.
15. Hirt, C.W. and Nichols, B.D., *J. Comput. Phys.*, 1981, no. 39, p. 201.
16. Degtiar, V.G., Pegov, V.I., Moshkin, I.Yu., and Cheshko, A.D., *High Temp.*, 2019, vol. 57, no. 5, p. 707.
17. Khabakhpasheva, E.M. and Perepelitsa, B.V., *J. Eng. Phys.*, 1968, vol. 14, no. 4, p. 319.
18. Adrian, R.J., *Ann. Rev. Fluid Mech.*, 1991, vol. 23, p. 261.
19. Raffel, M., Willert, C., Kompenhans, J., and Werely, S., *Particle Image Velocimetry: A Practical Guide*, Berlin: Springer, 2007, 2nd ed.
20. Elsinga, G.E., Scarano, F., Wieneke, B., and van Oudheusden, B.W., *Exp. Fluids*, 2006, vol. 41, p. 933.
21. Scarano, F., *Meas. Sci. Technol.*, 2013, vol. 24, 012001.
22. Alekseenko, S.V., Dulin, V.M., Kozorezov, Y.S., and Markovich, D.M., *Int. J. Heat Fluid Flow*, 2008, vol. 29, p. 1699.
23. Alekseenko, S.V., Antipin, V.A., Cherdantsev, A.V., Kharlamov, S.M., and Markovich, D.M., *Phys. Fluids*, 2009, vol. 21, 061701.
24. Shestakov, M.V., Tokarev, M.P., and Markovich, D.M., *Sci. Visualization*, 2015, vol. 7, no. 3, p. 1.
25. Alekseenko, S.V., Dulin, V.M., Tokarev, M.P., and Markovich, D.M., *Thermophys. Aeromech.*, 2016, vol. 23, no. 2, p. 301.

26. Alekseenko, S.V., Abdurakipov, S.S., Hrebtov, M.Y., Tokarev, M.P., Dulin, V.M., and Markovich, D.M., *Int. J. Heat Fluid Flow*, 2018, vol. 70, p. 363.
27. Varaksin, A.Yu., Mikhatulin, D.S., Polezhaev, Yu.V., and Polyakov, A.F., *High Temp.*, 1995, vol. 33, no. 6, p. 911.
28. Varaksin, A.Yu., Polezhaev, Yu.V., and Polyakov, A.F., *High Temp.*, 1998, vol. 36, no. 5, p. 744.
29. Varaksin, A.Yu., Polezhaev, Yu.V., and Polyakov, A.F., *Int. J. Heat Fluid Flow*, 2000, vol. 21, no. 5, p. 562.
30. Varaksin, A.Yu. and Ivanov, T.F., *High Temp.*, 2004, vol. 42, no. 1, p. 73.
31. Pakhomov, M.A., Protasov, M.V., Terekhov, V.I., and Varaksin, A.Yu., *Int. J. Heat Mass Transfer*, 2007, vol. 50, p. 2107.
32. Varaksin, A.Yu., *High Temp.*, 2015, vol. 53, no. 3, p. 423.
33. Varaksin, A.Yu., *High Temp.*, 2019, vol. 57, no. 4, p. 555.
34. Akhmetbekov, Y.K., Alekseenko, S.V., Dulin, V.M., Markovich, D.M., and Pervunin, K.S., *Exp. Fluids*, 2010, vol. 48, p. 615.
35. Alekseenko, S., Cherdantsev, A., Cherdantsev, M., Isaenkov, S., Kharlamov, S., and Markovich, D., *Exp. Fluids*, 2012, vol. 53, no. 1, p. 77.
36. Polezhaev, Yu.V. and Yurevich, F.B., *Teplovaya zashchita* (Thermal Protection), Moscow: Energiya, 1976.
37. Polezhaev, Yu.V. and Shishkov, A.A., *Gazodinamicheskie ispytaniya teplovoi zashchity. Spravochnik* (Gas-Dynamic Tests of Thermal Protection: Handbook), Moscow: Promedek, 1992.
38. Mikhatulin, D.S., Polezhaev, Yu.V., and Reviznikov, D.L., *Teploobmen i razrushenie tel v sverkhzvukovom geterogennom potoke* (Heat Transfer and Destruction of Bodies in Supersonic Heterogeneous Flow), Moscow: Yanus-K, 2007.
39. Mikhatulin, D.S., Polezhaev, Yu.V., and Reviznikov, D.L., *Teplomassoobmen. Termokhimicheskoe i termoerozionnoe razrushenie teplovoi zashchity* (Heat and Mass Transfer: Thermochemical and Thermoerosive Destruction of Thermal Protection), Moscow: Yanus-K, 2011.
40. Nikitin, P.V., *Teplovaya zashchita. Uchebnik dlya vysshei shkoly* (Thermal Protection: Textbook), Moscow: Mosk. Aviats. Inst., 2006.
41. Afanasyev, V.A., Nikitin, P.V., and Tushavina, O.V., *High Temp.*, 2019, vol. 57, no. 4, p. 525.
42. Strakhov, V.L., Kuz'min, I.A., and Bakulin, V.N., *High Temp.*, 2019, vol. 57, no. 2, p. 250.
43. Mironov, V.V. and Tolkach, M.A., *High Temp.*, 2019, vol. 57, no. 2, p. 242.
44. Astapov, A.N., Lifanov, I.P., and Rabinskii, L.N., *High Temp.*, 2019, vol. 57, no. 5, p. 744.
45. Zhestkov, B.E., Vaganova, M.L., Lebedeva, Yu.E., Sorokin, O.Yu., and Medvedev, P.N., *High Temp.*, 2018, vol. 56, no. 3, p. 378.
46. Zinchenko, V.I., Gol'din, V.D., and Zverev, V.G., *High Temp.*, 2018, vol. 56, no. 5, p. 719.
47. Dombrovsky, L.A., Reviznikov, D.L., and Sposobin, A.V., *Int. J. Heat Mass Transfer*, 2016, vol. 93, p. 853.
48. Reviznikov, D.L., Sposobin, A.V., and Dombrovsky, L.A., *Comput. Therm. Sci.*, 2015, vol. 7, no. 4, p. 313.
49. Reviznikov, D.L., Sposobin, A.V., and Ivanov, I.E., *High Temp.*, 2018, vol. 56, no. 6, p. 884.
50. Reviznikov, D.L., Sposobin, A.V., and Ivanov, I.E., *High Temp.*, 2020, vol. 58, no. 2, p. 280.
51. Vatazhin, A.B., Grabovskii, V.I., and Likhter, V.A., *Elektrogazodinamicheskie techeniya* (Electro-Gas-Dynamic Flows), Moscow: Nauka, 1983.
52. Rudinskii, A.V. and Yagodnikov, D.A., *High Temp.*, 2019, vol. 57, no. 5, p. 753.
53. Varaksin, A.Yu., Romash, M.E., and Kopeitsev, V.N., *High Temp.*, 2010, vol. 48, no. 4, p. 588.
54. Varaksin, A.Y., Romash, M.E., and Kopeitsev, V.N., *AIP Conf. Proc.*, 2010, vol. 1207, p. 342.
55. Varaksin, A.Yu., Romash, M.E., Kopeitsev, V.N., and Gorbachev, M.A., *Int. J. Heat Mass Transfer*, 2012, vol. 55, p. 6567.
56. Varaksin, A.Yu., Romash, M.E., Kopeitsev, V.N., and Gorbachev, M.A., *High Temp.*, 2011, vol. 49, no. 2, p. 310.
57. Varaksin, A.Yu., Romash, M.E., Kopeitsev, V.N., and Gorbachev, M.A., *High Temp.*, 2010, vol. 48, no. 6, p. 918.
58. Varaksin, A.Yu., Protasov, M.V., and Teplitskii, Yu.S., *High Temp.*, 2014, vol. 52, no. 4, p. 554.
59. Varaksin, A.Yu., *High Temp.*, 2017, vol. 55, no. 2, p. 286.
60. Varaksin, A.Yu. and Zaichik, L.I., *High Temp.*, 1998, vol. 36, no. 6, p. 983.
61. Zaichik, L.I. and Varaksin, A.Yu., *High Temp.*, 1999, vol. 37, no. 4, p. 655.
62. Varaksin, A.Yu., Romash, M.E., and Kopeitsev, V.N., *High Temp.*, 2009, vol. 47, no. 6, 836.
63. Varaksin, A.Yu., Romash, M.E., and Kopeitsev, V.N., *High Temp.*, 2010, vol. 48, no. 3, p. 411.
64. Pokhil, P.F., Belyaev, A.F., Frolov, Yu.V., Logachaev, V.S., and Korotkov, A.I., *Gorenie poroshkoobraznykh metallov v aktivnykh sredakh* (Combustion of Powdered Metals in Active Media), Moscow: Nauka, 1972.
65. Mitrofanov, V.V., *Detonatsiya gomogennykh i geterogennykh system* (Detonation of Homogeneous and Heterogeneous Systems), Novosibirsk: Inst. Gidrodin. im. M.A. Lavrent'eva, Sib. Otd. Ross. Akad. Nauk, 2003.
66. Fedorov, A.V., Fomin, V.M., and Khmel', T.A., *Volnovye protsessy v gazovzvesyakh chastits metallov* (Wave Processes in Gas-Suspended Particles of Metals), Novosibirsk: Parallel', 2015.
67. Fedorov, A.V. and Khmel, T.A., *Combust., Explos. Shock Waves (Engl. Transl.)*, 2019, vol. 55, no. 1, p. 1.
68. Lenkevich, D.A., Golovastov, S.V., Golub, V.V., Bocharnikov, V.M., and Bivol, G.Yu., *High Temp.*, 2014, vol. 52, no. 6, p. 890.
69. Bivol, G.Yu., Golovastov, S.V., and Golub, V.V., *High Temp.*, 2017, vol. 55, no. 4, p. 561.
70. Mirova, O.A., Bazhenova, T.V., and Golub, V.V., *High Temp.*, 2020, vol. 58, no. 1, p. 140.
71. Gidaspov, V.Yu. and Severina, N.S., *High Temp.*, 2019, vol. 57, no. 4, p. 514.
72. Mednikov, E.P., *Akusticheskaya koagulyatsiya i osazhdenie aerozolei* (Acoustic Coagulation and Deposition of Aerosols), Moscow: Akad. Nauk SSSR, 1963.
73. Gubaidullin, D.A., Zaripov, R.G., Tkachenko, L.A., and Shaidullin, L.R., *High Temp.*, 2019, vol. 57, no. 2, p. 283.

74. Gubaidullin, D.A., Zaripov, R.G., Tkachenko, L.A., and Shaidullin, L.R., *High Temp.*, 2019, vol. 57, no. 5, p. 768.
75. Gubaidullin, D.A., Teregulova, E.A., and Gubaidullina, D.D., *High Temp.*, 2019, vol. 57, no. 3, p. 414.
76. Gubaidullin, D.A. and Zaripov, R.R., *High Temp.*, 2019, vol. 57, no. 3, p. 444.
77. Gubaidullin, D.A. and Zaripov, R.R., *High Temp.*, 2019, vol. 57, no. 4, p. 600.
78. Devisilov, V.A. and Sharai, E.Yu., *High Temp.*, 2018, vol. 56, no. 4, p. 576.
79. Frishberg, I.V., Kvater, L.I., Kuz'min, B.P., and Gribovskii, S.V., *Gazofaznyi metod polucheniya poroshkov* (Gas-Phase Method for Producing Powders), Moscow: Nauka, 1978.
80. Woehl, T.J., Park, C., Evans, J.E., Arslan, I., Ristenpart, W.D., and Browning, N.D., *Nano Lett.*, 2014, vol. 14, p. 373.
81. Varaksin, A.Yu., *High Temp.*, 2014, vol. 52, no. 5, p. 752.
82. Smirnov, B.M., *Phys.—Usp.*, 2011, vol. 54, no. 7, p. 691.
83. Korenchenko, A.E., Vorontsov, A.G., Gel'chinskii, B.R., and Zhukova, A.A., *High Temp.*, 2019, vol. 57, no. 2, p. 275.
84. Vorontsov, A.G., Korenchenko, A.E., and Gel'chinskii, B.R., *High Temp.*, 2019, vol. 57, no. 3, p. 368.
85. Zalkind, V.I., Zeigarnik, Yu.A., Nizovskiy, V.L., Nizovskiy, L.V., and Shchigel, S.S., *High Temp.*, 2018, vol. 56, no. 1, p. 153.
86. Alekseev, V.B., Zalkind, V.I., Ivanov, P.P., Nizovskiy, V.L., and Schigel, S.S., *High Temp.*, 2019, vol. 57, no. 4, p. 547.
87. Alekseev, V.B., Zalkind, V.I., Nizovskii, V.L., Nizovskii, L.V., Khyamyalyainen, L.T., and Shchigel', S.S., *High Temp.*, 2018, vol. 56, no. 3, p. 418.
88. Nazarov, A.D., Serov, A.F., and Terekhov, V.I., *High Temp.*, 2011, vol. 49, no. 1, p. 116.
89. Nazarov, A.D., Serov, A.F., and Terekhov, V.I., *High Temp.*, 2014, vol. 52, no. 4, p. 576.
90. Deich, M.E. and Filippov, G.A., *Gazodinamika dvukhfaznykh sred* (Gas Dynamics of Two-Phase Media), Moscow: Energoizdat, 1981.
91. Chen, K.S., Hicker, M.A., and Noble, D.R., *Int. J. Energy Res.*, 2005, vol. 29, p. 1113.
92. Theodorakakos, A., Ous, T., Gavaises, M., Nouri, J.M., Nikolopoulos, N., and Yanagihara, H., *J. Colloid Interface Sci.*, 2006, vol. 300, p. 673.
93. Varaksin, A.Yu., *High Temp.*, 2018, vol. 56, no. 2, p. 275.
94. Grinats, E.S., Zhbanov, V.A., Kashevarov, A.V., Miller, A.B., Potapov, Yu.F., and Stasenko, A.L., *High Temp.*, 2019, vol. 57, no. 2, p. 222.
95. Kutateladze, S.S., Volchkov, E.P., and Terekhov, V.I., *Aerodinamika i teplomassoobmen v ogranichennykh vikhrevykh potokakh* (Aerodynamics and Heat and Mass Transfer in Limited Vortex Flows), Novosibirsk: Sib. Otd. Ross. Akad Nauk, 1987.
96. Gupta, A.K., Lilley, D.G., and Syred, N., *Swirl Flows*, Tunbridge Wells: Abacus, 1984.
97. Khalatov, A.A., *Teoriya i praktika zakruchennykh potokov* (Theory and Practice of Swirl Flows), Kiev: Naukova Dumka, 1989.
98. Pakhomov, M.A. and Terekhov, V.I., *High Temp.*, 2018, vol. 56, no. 3, p. 410.
99. Zel'dovich, Ya.B., *Teoriya goreniya i detonatsii gazov* (Theory of Gas Combustion and Detonation), Moscow: Akad. Nauk SSSR, 1944.
100. Chernyi, G.G., *Gazovaya dinamika* (Gas Dynamics), Moscow: Nauka, 1988.
101. Mitrofanov, V.V., *Detonatsiya gomogennykh i geterogennykh system* (Detonation of Homogeneous and Heterogeneous Systems), Novosibirsk: Inst. Gidrodin. im. M.A. Lavrent'eva, Sib. Otd. Ross. Akad. Nauk, 2003.
102. Pirumov, U.G., *Matematicheskoe modelirovanie v problemakh okhrany vozdushnogo basseina* (Mathematical Simulation in Problems of Air Basin Protection), Moscow: Mosk. Aviats. Inst., 2001.
103. Gidaspov, V.Yu., Moskalenko, O.A., and Severina, N.S., *High Temp.*, 2018, vol. 56, no. 5, p. 751.
104. Gubaidullin, D.A., Zaripov, R.G., Tkachenko, L.A., and Shaidullin, L.R., *High Temp.*, 2018, vol. 56, no. 1, p. 146.
105. Gubaidullin, D.A. and Teregulova, E.A., *High Temp.*, 2018, vol. 56, no. 5, p. 758.
106. Gubaidullin, D.A. and Tukmakov, D.A., *High Temp.*, 2019, vol. 57, no. 6, p. 899.
107. Tukmakov, A.L. and Tukmakova, N.A., *High Temp.*, 2019, vol. 57, no. 3, p. 398.
108. Struleva, E.V., Komarov, P.S., and Ashitkov, S.I., *High Temp.*, 2018, vol. 56, no. 5, p. 648.
109. Struleva, E.V., Komarov, P.S., and Ashitkov, S.I., *High Temp.*, 2019, vol. 57, no. 4, p. 486.
110. Struleva, E.V., Komarov, P.S., and Ashitkov, S.I., *High Temp.*, 2019, vol. 57, no. 5, p. 659.
111. Rusanov, A.I., *Fazovye ravnovesiya i poverkhnostnye yavleniya* (Phase Equilibria and Surface Phenomena), Leningrad: Khimiya, 1967.
112. Lushnikov, A.A., *Dokl. Akad. Nauk SSSR*, 1977, vol. 234, p. 97.
113. Tovbin, Yu.K. and Zaitseva, E.S., *High Temp.*, 2018, vol. 56, no. 3, p. 366.
114. Kovaleva, L.A., Minnigalimov, R.Z., and Zinnatullin, R.R., *Energy Fuels*, 2011, vol. 25, no. 8, p. 3731.
115. Kovaleva, L.A., Minnigalimov, R.Z., and Zinnatullin, R.R., *High Temp.*, 2008, vol. 46, no. 5, p. 728.
116. Fang, C.S. and Lai, M.C., in *Proc. 14th National Industrial Energy Technology Conf.*, Houston, TX, 1992, p. 125.
117. Abdurahman, H.N., Rosli, M.Y., and Azhary, H.N., *World Acad. Sci., Eng. Technol.*, 2010, vol. 62, p. 188.
118. Kovaleva, L.A., Zinnatullin, R.R., Mullayanov, A.I., Mavletov, M.V., and Blagochinnov, V.N., *High Temp.*, 2013, vol. 51, no. 6, p. 870.
119. Kovaleva, L.A., Zinnatullin, R.R., Minnigalimov, R.Z., Blagochinnov, V.N., and Mullayanov, A.I., *Neftepromysl. Delo*, 2013, no. 6, p. 45.
120. Kovaleva, L.A., Musin, A.A., and Fatkhullina, Yu.I., *High Temp.*, 2018, vol. 56, no. 2, p. 234.
121. Mudawar, I. and Bowers, H.B., in *Convective Flow Boiling*, Chen, J.C., Ed., New York: Tailor & Francis, 1995, p. 117.
122. Vasil'ev, N.V., Zeigarnik, Yu.A., Khodakov, K.A., and Fedulenkov, V.M., *High Temp.*, 2015, vol. 53, no. 6, p. 837.
123. Kim, D.E., Yu, D.I., Jerng, D.W., Kim, M.H., and Ahn, H.S., *Exp. Therm. Fluid Sci.*, 2015, vol. 66, p. 173.

124. Vasil'ev, N.V., Varaksin, A.Yu., Zeigarnik, Yu.A., Khodakov, K.A., and Epel'fel'd, A.V., *High Temp.*, 2017, vol. 55, no. 6, p. 880.
125. Serdyukov, V.S., Surtaev, A.S., Pavlenko, A.N., and Chernyavskiy, A.N., *High Temp.*, 2018, vol. 56, no. 4, p. 546.
126. Dedov, A.V., Zabirov, A.R., Sliva, A.P., Fedorovich, S.D., and Yagov, V.V., *High Temp.*, 2019, vol. 57, no. 1, p. 63.
127. Sirotkina, A.L., Fedorovich, E.D., and Sergeev, V.V., *High Temp.*, 2018, vol. 56, no. 5, p. 732.
128. Ota, T., *Appl. Mech. Rev.*, 2000, vol. 53, p. 219.
129. Terekhov, V.I., Yarygina, N.I., and Zhdanov, R.F., *Int. J. Heat Mass Transfer*, 2003, vol. 46, p. 4535.
130. Pakhomov, M.A. and Terekhov, V.I., *High Temp.*, 2018, vol. 56, no. 1, p. 52.
131. Pakhomov, M.A. and Terekhov, V.I., *High Temp.*, 2019, vol. 57, no. 1, p. 89.
132. Woezel, J.L. and Ewing, M., Explosion sounds in shallow water, in *Propagation of Sound in the Ocean*, New York: Geol. Soc. Am., 1948, vol. 27.
133. Brekhovskikh, L.M., *Volny v sloistykh sredakh* (Waves in Layered Media), Moscow: Nauka, 1975.
134. Brekhovskikh, L.M. and Lysanov, Yu.P., *Teoreticheskie osnovy akustiki okeana* (Theoretical Foundations of Ocean Acoustics), Leningrad: Gidrometeoizdat, 1982.
135. Nigmatulin, R.I., Shagapov, V.Sh., Gimaltdinov, I.K., and Galimzyanov, M.N., *Dokl. Phys.*, 2001, vol. 46, p. 445.
136. Shagapov, V.Sh., Galimzyanov, M.N., and Vdovenko, I.I., *High Temp.*, 2019, vol. 57, no. 2, p. 256.
137. Shagapov, V.Sh., Galimzyanov, M.N., and Vdovenko, I.I., *High Temp.*, 2019, vol. 57, no. 3, p. 425.
138. Shagapov, V.Sh., Galimzyanov, M.N., and Vdovenko, I.I., *High Temp.*, 2019, vol. 57, no. 5, p. 712.
139. Rayleigh, L., *Philos. Mag.*, 1917, vol. 34, no. 200, p. 94.
140. Zel'dovich, Ya.B. and Raizer, Yu.P., *Fizika udarnykh voln i vysokotemperaturnykh gidrodinamicheskikh yavlenii* (Physics of Shock Waves and High-Temperature Hydrodynamic Phenomena), Moscow: Nauka, 1966.
141. Hunter, C., *J. Fluid Mech.*, 1960, vol. 8, no. 2, p. 241.
142. Zababakhin, E.I. and Zababakhin, I.E., *Yavleniya neogranichennoi kumulyatsii* (Phenomena of Unlimited Cumulation), Moscow: Nauka, 1988.
143. Brushlinskii, K.V. and Kazhdan, Ya.M., *Usp. Mat. Nauk*, 1963, vol. 18, no. 2, p. 3.
144. Kraiko, A.N., *Prikl. Mat. Mekh.*, 2007, vol. 71, no. 5, p. 744.
145. Il'mov, D.N. and Cherkasov, S.G., *High Temp.*, 2012, vol. 50, no. 5, p. 631.
146. Morenko, I.V., *High Temp.*, 2019, vol. 57, no. 5, p. 718.
147. Sychev, A.I., *Combust., Explos. Shock Waves (Engl. Transl.)*, 1985, vol. 21, p. 250.
148. Sychev, A.I., *Combust., Explos. Shock Waves (Engl. Transl.)*, 1985, vol. 21, p. 365.
149. Kuznetsov, N.M. and Kopotev, V.A., *Dokl. Akad. Nauk SSSR*, 1989, vol. 304, no. 4, p. 850.
150. Zhdan, S.A., *Combust., Explos. Shock Waves (Engl. Transl.)*, 2002, vol. 38, p. 327.
151. Nigmatulin, R.I., Shagapov, V.Sh., Gimaltdinov, I.K., and Akhmadullin, F.F., *Dokl. Phys.*, 2003, vol. 48, no. 2, p. 75.
152. Nigmatulin, R.I., Shagapov, V.Sh., Gimaltdinov, I.K., and Bayazitova, A.R., *Dokl. Phys.*, 2005, vol. 50, p. 405.
153. Sychev, A.I., *Tech. Phys.*, 2017, vol. 87. Vyp. 4, p. 523.
154. Sychev, A.I., *High Temp.*, 2019, vol. 57, no. 2, p. 263.
155. Gimaltdinov, I.K. and Lepikhin, S.A., *High Temp.*, 2019, vol. 57, no. 3, p. 420.
156. Nigmatulin, R.I., Aganin, A.A., Il'gamov, M.A., and Toporkov, D.Yu., *High Temp.*, 2019, vol. 57, no. 2, p. 228.
157. Bennet, R.J., in *Water and Water Pollution Handbook*, Ciaccio, L.L., Ed., New York: Marcel Dekker, 1971, p. 261.
158. Babaeva, N.YU., Berry, R.S., Naidis, G.V., Smirnov, B.M., Son, E.E., and Tereshonok, D.V., *High Temp.*, 2016, vol. 54, no. 5, p. 745.
159. Smirnov, B.M., Babaeva, N.Yu., Naidis, G.V., Panov, V.A., Son, E.E., and Tereshonok, D.V., *High Temp.*, 2019, vol. 57, no. 2, p. 286.
160. Degtyar', V.G. and Pegov, V.I., *Gidrodinamika podvodnogo starta raket* (Hydrodynamics of Underwater Rocket Launch), Moscow: Mashinostroenie, 2009.

Translated by E. Oborin